Scripta Materialia 141 (2017) 89–93

Contents lists available at ScienceDirect

Scripta Materialia

journal homepage: www.elsevier.com/locate/scriptamat

Regular article

Microstructure and its influence on thermoelectric properties of hot-extruded Bi-Sb-Te bulk materials

Zhi-Lei Wang, Takehiro Araki, Tetsuhiko Onda, Zhong-Chun Chen *

Department of Mechanical and Aerospace Engineering, Graduate School of Engineering, Tottori University, Koyama-minami 4-101, Tottori 680-8552, Japan

ARTICLE INFO

Article history:
Received 26 May 2017
Received in revised form 27 July 2017
Accepted 27 July 2017
Available online xxxx

Keywords:
Bismuth telluride
Microstructure
Twinning
Thermoelectric properties
Extrusion

ABSTRACT

The microstructural features and relationships among extrusion temperature, microstructure, and thermoelectric/mechanical properties of hot-extruded $Bi_{0.4}Sb_{1.6}Te_3$ materials have been investigated. The microstructure was characterized by fine and equiaxed grains with many twin boundaries and preferred orientation of {0001}. A twin pair shared a certain {0001} basal plane as the twin plane and had an orientation relationship of 60° or 180° rotation about *c*-axis. The sample extruded at higher temperature exhibited higher fractions of small-angle grain boundaries and twin boundaries due to formation of Te-rich and Sb-rich phases. The higher fraction of twin boundaries caused a reduction in phonon thermal conductivity.

Bi_2Te_3-based thermoelectric materials are extensively used in various electronic devices of cooling and temperature control. The conversion efficiency of a thermoelectric device is determined by the materials' dimensionless figure of merit (ZT), defined as $ZT = \alpha^2 T / (\rho\kappa)$, where α, ρ, κ, and T are the Seebeck coefficient, electrical resistivity, thermal conductivity, and absolute temperature, respectively.

Bi_2Te_3 compound has a layered rhombohedral structure with atomic layer series in the order of -Te(1)-Bi-Te(2)-Bi-Te(1)- along the *c*-axis [1,2]. The Te and Bi atoms are connected by strong covalent or ionic bonds, while Te(1)–Te(1) layers are weakly bound by the van der Waals forces [2], which easily result in cleavage in the direction parallel to the basal planes. This crystal structure also exhibits anisotropy with respect to electrical and thermal transport properties [3].

In the recent decades, a lot of efforts have been made to improve the performance of Bi_2Te_3-based thermoelectric materials [4–11]. Microstructural control, as acknowledged, is one of the important ways to enhance the thermoelectric and mechanical performance of polycrystalline Bi_2Te_3-based materials. For example, low thermal conductivity can be obtained by reducing grain size because of increased phonon scattering at high-density grain boundaries [8–11]. And electrical conductivity can be improved by introducing texture because electrical conductivity has high anisotropy. For instance, the electrical conductivity is much higher in the directions parallel to the basal plane than to the *c*-axis [12]. In addition, small grain size is also beneficial to the materials' mechanical strength.

In the present work, from the viewpoints of grain refinement and preferred orientation, mechanical alloying (MA) and hot-extrusion technique was proposed to fabricate Bi-Sb-Te bulk materials. The microstructural features including grain size, orientation, grain- and twin-boundary characteristics in Bi-Sb-Te bulk materials hot-extruded at different temperatures were investigated. The purpose of the current work was to further understand the relationships among extrusion temperature, microstructure/texture, and thermoelectric/mechanical properties as well as improve the performance of Bi_2Te_3-based materials through microstructure control.

High purity Bi, Sb, and Te (>99.9% purity) powders were used as the starting materials. The starting powders with a nominal composition of $Bi_{0.4}Sb_{1.6}Te_3$ were subjected to MA under 200 rpm for 24 h in a purified argon atmosphere. The MAed powders were uniaxially pressed into a cylindrical green compact, followed by hot extrusion at two representative temperatures: 340 °C and 400 °C. From our previous work [13], the former results in fine-grained microstructure, while the latter has been demonstrated to be an optimal extrusion temperature for preparing Bi-Te-Se bulk materials with good thermoelectric and mechanical properties. Besides, an extrusion ratio of 25:1 and a punch speed of 1 mm/min were used in the experiments.

Phase identification was performed by X-ray diffraction (XRD) with Cu Kα radiation. The microstructures were observed using scanning electron microscopy (SEM) and compositional analyses were conducted by electron probe micro-analyzer (EPMA) and energy dispersive X-ray spectroscopy (EDS). Orientation imaging microscopy (OIM) analysis was performed using an SEM equipped with an electron backscattered diffraction (EBSD) system. The electronic transport properties were evaluated by a Hall effect measurement system (Resi Test 8300, TOYO

* Corresponding author.
E-mail address: chen@mech.tottori-u.ac.jp (Z.-C. Chen).

http://dx.doi.org/10.1016/j.scriptamat.2017.07.032
1359-6462/

Corp.). The Seebeck coefficient (α) and electrical resistivity (ρ) of the samples were simultaneously measured by static DC method and four-probe method, respectively, using a thermoelectric property test apparatus (ZEM-3, ULVAC-RIKO). The thermal conductivity (κ) was measured by laser flash method (LFA457 Micro Flash, NETZSCH). All the thermoelectric properties were measured at 300 K. The dimensionless figure of merit of the samples was calculated by the equation of $ZT = \alpha^2 T / (\rho\kappa)$. In addition, the mechanical properties at room temperature were evaluated by the Vickers hardness test at a load of 1.96 N (HMV-2000, Shimadzu).

Fig. 1(a) and (b) shows the SEM backscattered electron images of the longitudinal sections (parallel to extrusion direction) of the extruded samples. Three regions with different contrasts, white, grey, and dark, were observed in both samples. For the sample extruded at 340 °C (Fig. 1(a)), small-sized grey and dark regions were homogeneously distributed in white matrix. At 400 °C, however, some grey regions became quite larger in addition to small grey phase. EPMA compositional analysis corresponding to the square area in Fig. 1(b) indicated that the grey regions were Te-rich and some dark regions were Sb-rich, as shown in Fig. 1(c). EDS quantitative analysis showed that the composition of the white matrix was close to the nominal composition of $Bi_{0.4}Sb_{1.6}Te_3$, while that of some grey regions had a Te content as high as 97 at.%. It has been demonstrated in our previous work [14] that the formation of small and large Te-rich phase is attributed to sublimation of Te and eutectic reaction, respectively. Concurrent with the loss of Te, the amount of Sb in some regions became higher, i.e., Sb-rich phase appeared. In addition to Sb-rich phase, a lot of dark points are considered to result from pores remained in the samples after hot extrusion.

Fig. 2(a) and (b) shows the inverse pole figure (IPF) maps of the longitudinal sections of the extruded samples, revealing morphology, size, and orientation of the grains. The microstructures were characterized by fine and equiaxed grains with many twin boundaries (TBs, expressed by black lines). These fine and equiaxed grains are attributed to dynamic recrystallization during the extrusion and static recrystallization after extrusion [15]. As the extrusion temperature increased, obvious grain growth occurred, for example, the average grain sizes were measured to be 0.37 μm and 0.65 μm with standard deviations of 0.19 μm and 0.49 μm for the samples extruded at 340 °C and 400 °C, respectively. Moreover, both XRD and EBSD analyses demonstrated that {0001} basal planes in the extruded samples were preferentially oriented parallel to the extrusion direction. For example, the orientation factors of the basal planes $f_{(0001)}$, calculated from XRD data using the Lotgering method [16], were 0.225 and 0.221 at 340 °C and 400 °C, respectively. This indicates that there is no significant difference in crystal orientation in both samples extruded at 340 °C and 400 °C.

It should be noted that the crystal structures of the Te-rich and Sb-rich phases shown in Fig. 1 are different from $Bi_{0.4}Sb_{1.6}Te_3$. Such second phases have a low confidence index (CI) of <0.1 in the EBSD analysis, which causes some trouble to identify their crystal structures and corresponding orientations. It has been reported that EBSD patterns with CI > 0.1 can correctly index a crystal orientation at 95% [17]. In the current work, the average CIs of the patterns were >0.53, which led to >99.9% of the patterns being indexed correctly, indicating high reliability [18]. Thus, it seems reasonable that the effect of Te-rich and Sb-rich phases on IPF maps of $Bi_{0.4}Sb_{1.6}Te_3$ can be ignored.

The grain-boundary maps corresponding to the IPF maps in Fig. 2(a) and (b) are shown in Fig. 2(c) and (d), respectively. The misorientation angle was divided into 2–5°, 5–15°, and >15° which were drawn by red, green, and blue lines, respectively. Almost all the boundaries were identified as large-angle grain boundaries (LAGBs, blue lines) because of dynamic and static recrystallization, although small amount of small-angle grain boundaries (SAGBs) existed inside some grains. It is interesting to note that the fraction of SAGBs in the sample extruded at 400 °C (13.8%, expressed by boundary length) is larger than that in the sample extruded at 340 °C (8.9%). This may be associated with the increased Te-rich and Sb-rich phases that inhibited the movement of the SAGBs as demonstrated in our previous work [19].

As is well known, kernel average misorientation (KAM) analysis can evaluate local lattice distortion, localized deformation, and dislocation density within a given region [20]. Fig. 2(e) and (f) shows the KAM maps corresponding to the boundary maps, revealing local lattice distortion distributions in the extruded samples. The local distortion was distributed inhomogeneously among the grains in both samples, but the area with quite low KAM value approaching to 0° (expressed by blue color) became larger in the sample extruded at 400 °C compared to the sample extruded at 340 °C. This suggests that there are a lower residual dislocation density and less local distortion in the sample extruded at 400 °C, which can cause an increase in thermal conductivity. The average KAM values were measured to be 0.51° and 0.46° for the sample extruded at 340 °C and 400 °C, respectively. Moreover, in comparison

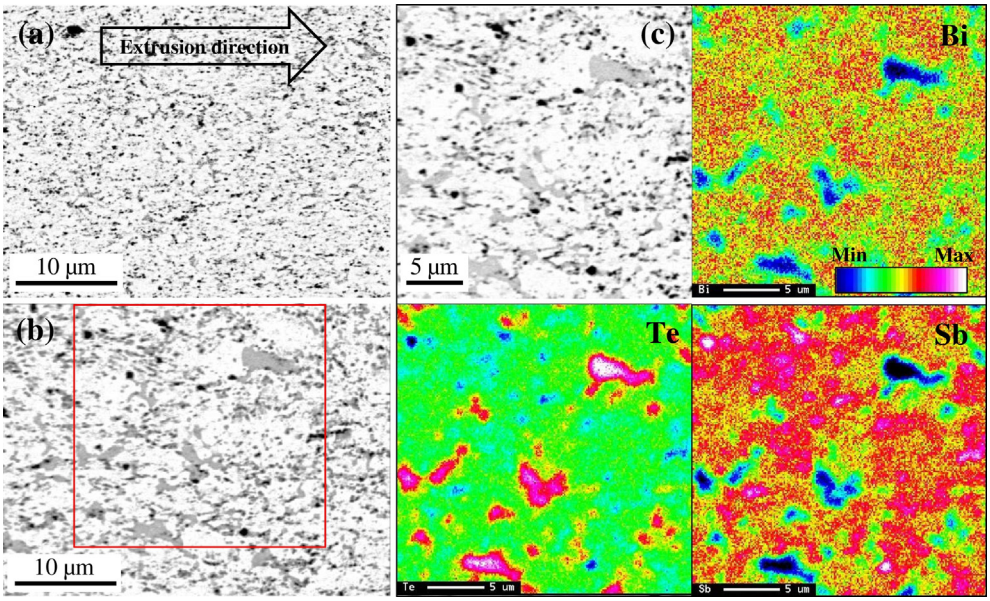

Fig. 1. SEM backscattered electron images of the samples extruded at (a) 340 °C and (b) 400 °C. (c) EPMA maps corresponding to the square area marked in (b).